

# Model Identification and Physical Exercise Control using Nonlinear Heart Rate Model and Particle Filter\*

Dongping Du, Zhiyong Hu, Yuncheng Du, *Member, IEEE*

**Abstract**— Physical exercise has been proven to be beneficial for both healthy subjects and cardiac patients. It can improve cardiovascular health and promote recovery from various heart conditions. Heart Rate (HR) is a cardiovascular variable, which can be easily monitored and provides important insights about cardiac functions during and after physical exercise. This study presents a HR-based modeling and control framework to monitor physiological changes during exercise, from which the exercise intensity is optimized to capitalize exercise outcomes. HR models were previously developed to investigate exercise physiology, but efficient model identification has not been extensively discussed in the literature. Most existing HR models are nonlinear state-space models, and traditional optimization techniques may fail to provide accurate model identification results. In this work, we propose to use particle filter (PF) to identify HR model parameters and further optimize the intensity of exercise, e.g., walking or running speed, based on the calibrated model. Specifically, sequential importance sampling and resampling (SISR) and smoothing were chosen to estimate state variables, and particle marginal Metropolis-Hastings method was used to identify model parameters from HR observations. In addition, using predictions calculated from the HR model, treadmill speed was optimized by minimizing the difference between predictions and the target HR. The modeling and control framework is validated with different case studies. The results demonstrate that the proposed method is a useful tool for personalized HR modeling and exercise control, which can benefit both regular exercise training and cardiac rehabilitation.

## I. INTRODUCTION

Cardiovascular disease is the leading cause of death in the United States, and about 610,000 people die of heart disease every year, i.e., 1 in every 4 deaths [1, 2]. Regular physical activity helps decrease the chance of having a heart attack or stroke, and reduces the possibility of needing a coronary revascularization procedure [3]. Appropriate exercise training also benefits postoperative patients by promoting recovery. Cardiac output increases during physical exercise, which can consequently increase the volume of oxygen extracted from blood. However, it is important to monitor such changes to ensure normal and healthy cardiac responses with respect to different exercise intensities, thus preventing sudden cardiac events such as heart attack. Heart Rate (HR) is one of the cardiovascular variables that can be easily measured and used to gauge heart functions. Therefore, the analysis and modeling of HR during exercise has become an emerging topic. HR Models can provide a better understanding on exercise physiology, which reveals important insights for optimal

exercise control for both healthy subjects and cardiac patients. Studies have showed that the HR profile during exercise and recovery can be used as a predictor for sudden death [4]. For example, a blunted increase of HR at 40-100% of maximal workload during exercise was associated with increased cardiovascular mortality [5]. In addition, an accurate model of HR can be useful for monitoring exercise and suggesting optimal exercise intensity for maximized training outcomes.

Modeling of HR has been previously studied. Hajek et al studied the HR responses using feedforward and feedback components and estimated the model parameters in predefined small intervals for 15 healthy subjects [6]. Stirling et al developed a mathematical model to estimate HR responses during exercise, and used stochastic optimization algorithm to find optimal model parameters [7]. Zakynthinaki used two coupled ordinary differential equations (ODEs) to study HR during exercise. The model accounts for the rate of HR change and predicts HR responses based on exercise intensity, lactate accumulation, and subjects' overall cardiovascular condition [3]. Note that, parameters used in Zakynthinaki's model were determined empirically, and model identification was not discussed. Su et al built a HR model using Hammerstein system, which consists of a static nonlinearity cascade as the input of a linear system, and model parameters were identified using support vector regression with a regularized cost function [8]. In addition, Cheng et al introduced a nonlinear state-space model to predict the HR responses during and after treadmill walking exercise. As compared to other models, this model is efficient in describing both short and longer duration of exercises [9]. Cheng et al applied Levenberg–Marquardt method to estimate model parameters at different exercise intensities and HR responses. It is worth noting that state space model of HR response dominates the literature, which has been proven as an efficient approach to predict HR. However, few studies have discussed efficient parameter identification for state-space HR models.

Parameter identification for state-space HR models is challenging due to the model complexity and nonlinearity. For example, HR calculated from two state variables is regulated by two nonlinear differential equations in Cheng et al's model [9]. To obtain model parameters, estimation methods, such as least squares methods [10, 11], gradient-based methods [12, 13], and bias compensation methods [14, 15], can be used, which minimize the difference between the predicted HR and observations. However, HR data used for model calibration generally contain a significant amount of uncertainty such as noise and motion artifacts. Further, subjects are heterogeneous in baseline HR and exercise physiology. Without considering the uncertainty, model identification can be inefficient, which will result in inaccurate estimation of HR response and false control decision of exercise protocol design. Maximum

\*Research supported by National Science Foundation.

Dongping Du, and Zhiyong Hu are with the Department of Industrial, Manufacturing, and Systems Engineering, Texas Tech University, Lubbock, TX 79409 USA (corresponding author e-mail: dongping.du@ttu.edu)

Yuncheng Du is with the Department of Biomolecular and Chemical Engineering, Clarkson University, Potsdam, NY 13699, USA.

Likelihood Estimation (MLE) can be used to calibrate the model, while considering the measurement noise. However, the performance of MLE is suboptimal for state-space HR model, as the state variables and their initial values are often unknown. Kalman filter can be used in combination with MLE in order to obtain optimal parameters. However, Kalman filter is limited to linear Gaussian state-space model, thus providing less accurate results for nonlinear, non-Gaussian state-space HR model. As an alternative, Particle Filter (PF) is a sequential Monte Carlo method that estimate latent states in a dynamical system when only partial observations of HR are available in the presence of uncertainty. In this study, we propose to use particle method in combination with Bayesian parameter estimation to track HR variations and identify a set of optimal model parameters. Further, the calibrated model will be used to predict future HR and to identify best exercise intensities in order to meet exercise target and maximize training outcomes.

The rest of this paper is organized as follows. Section II briefly discusses the models and methods. Section III provides the experimental results, which is followed by discussions and conclusion in Section V.

## II. METHOD

### A. State-Space HR Response Model

In this study, Cheng et al's HR model is used to illustrate the proposed modeling and control framework [9]. To model HR variations with respect to different treadmill speeds, a nonlinear state-space control system was used [9]:

$$\dot{x}_1(t) = -a_1 x_1(t) + a_2 x_2(t) + a_3 u^2(t), \quad (1)$$

$$\dot{x}_2(t) = -a_4 x_2(t) + \phi(t), \quad (2)$$

$$y(t) = 4x_1(t) + 74, \quad (3)$$

$$\phi(t) = \frac{a_5 x_1(t)}{1 + \exp(-(x_1(t) - a_6))} \quad (4)$$

where  $s(0)$  is the initial condition and  $a_i, i = 1, \dots, 5$  is model parameter.  $y(t)$  is the HR response and  $u(t)$  is the treadmill speed. The 1<sup>st</sup> state variable  $x_1(t)$  describes the change of HR during exercise, while  $x_2(t)$  is the slower and more complex local peripheral effect [9]. For simplicity, we further write the state-space HR model as:

$$x_t = f_\theta(x_{t-1}) + w_t \quad (5)$$

$$y_t = g_\theta(x_t) + v_t \quad (6)$$

where  $\theta = \{a_i\}$ ,  $i = 1, 2, \dots, 6$ , is the model parameters,  $f_\theta$  is the nonlinear function that calculates the state value at  $t$  given  $x_{t-1}$ ,  $g_\theta$  is the function that calculates the observation at  $t$  given the state variable  $x_t$  and noises, i.e.,  $w_t \sim \mathcal{N}(0, Q)$ ,  $v_t \sim \mathcal{N}(0, R)$ .  $Q$  and  $R$  are covariances. Note that we assume HR data are corrupted with Gaussian noise in this study. However, other types of noise can be used, and the modeling and control follows the same procedure as explained below.

### B. Filtering

In this study, we choose to use Bayesian method to infer model parameters with a set of observations. One challenge for accurate parameter estimation is to infer state variables in the nonlinear state-space model based on HR observations, i.e.,  $y$  in (3). In this work, PF is used to obtain an estimation of the

internal variable  $x = \{x_0, \dots, x_n\}$ , given a set of known parameters and the observation  $y = \{y_0, \dots, y_n\}$ . The detailed procedures are discussed as follows.

Auxiliary particle filter, specifically sequential importance sampling and resampling (SISR), is used to estimate the states. The objective is to recursively characterize the joint posterior distributions  $\{p_\theta(x_n | y_{0:n})\}_{n \geq 0}$  through a sequence of data of HR. The posterior density of  $x_n$  given HR data  $y_{0:n-1}$  and the state transition density  $p(x_n | x_{n-1})$  can be calculated as [16]:

$$p_\theta(x_n | y_{0:n-1}) = \sum_{i=1}^N p(x_n | x_{n-1}^i) \pi_{n-1}^i \quad (7)$$

where  $\pi_{n-1}^i$  is the discrete probability mass of particles  $x_{n-1}^i$ ,  $N$  is the number of particles. Considering the measurement density at  $y_n$ , this can be written as [16]:

$$p_\theta(x_n | y_{0:n}) \propto p(y_n | x_n) \sum_{i=1}^N p(x_n | x_{n-1}^i) \pi_{n-1}^i \quad (8)$$

The samples of PF from (8) will produce new particles with weights of  $\pi$ . One can sample from  $p_\theta(x_n | y_{0:n-1})$  by choosing  $x_{n-1}^i$  with weights  $\pi_{n-1}^i$ , which can be obtained as [16]:

$$w_{n-1}^i = p(y_n | x_{n-1}^i), \quad \pi_{n-1}^i = \frac{w_{n-1}^i}{\sum_{j=1}^N w_{n-1}^j} \quad (9)$$

When  $n = 0$ , the weight can be obtained as [16]:

$$w_0 \propto p(y_0 | x_0) \pi_0$$

where  $\pi_0$  is a priori distribution of  $x_0$ . The posterior distribution of  $x_n$  at  $n$  is determined by the weighted sample  $(x_n^i, \pi_n^i)$ . The procedure of PF is summarized as follows [17].

---

For  $n = 0$ , for all  $i \in \{1, \dots, N\}$ :

1. Sample  $X_0^i \sim \pi_0(x_0 | y_0)$ .
2. Compute  $w_1^i \propto w_0(X_0^i)$ ,  $\pi_1^i = w_1^i / \sum_{j=1}^N w_1^j$ .
3. Resample  $\bar{X}_0^i \sim \sum_{j=1}^N \pi_1^j \delta(X_0 - X_0^j)$ .

For  $n = 1, 2, \dots, T$ , for all  $i \in \{1, \dots, N\}$ :

1. Sample  $X_n^i \sim p_\theta(x_n | y_n, \bar{X}_{n-1}^i)$ , set  $X_{0:n}^i \leftarrow \{\bar{X}_{n-1}^i, X_n^i\}$
2. Compute

$$w_{n+1}^i \propto w_n^i(X_{n-1:n}^i)$$

$$\pi_{n+1}^i = w_{n+1}^i / \sum_{j=1}^N w_{n+1}^j$$

3. Resample  $\bar{X}_n^i \sim \sum_{j=1}^N \pi_{n+1}^j \delta(X_n - X_n^j)$
- 

### C. Smoothing

Smoothing is used to estimate the distribution of state variables at the particular time given all the HR data up to some later time. Since additional HR data are incorporated in the estimation, the trajectory obtained in this procedure would be smoother. Given the posterior density of  $p_\theta(x_n | y_{0:n})$  described in previous section, the joint smoothing density  $p_\theta(x_{0:T} | y_{0:T})$  for  $T > n$  can be factorized as [18]:

$$p_\theta(x_{0:T} | y_{0:T}) = p_\theta(x_T | y_{0:T}) \prod_{n=0}^{T-1} p_\theta(x_n | y_{0:n}, x_{n+1}) \quad (10)$$

where  $p_\theta(x_n | y_{0:n}, x_{n+1})$  is a backward transition density given by [18]:



$$p_\theta(x_n|y_{0:n}, x_{n+1}) = \frac{p_\theta(x_{n+1}|x_n)p_\theta(x_n|y_{0:n})}{p_\theta(x_{n+1}|y_{0:n})} \quad (11)$$

$$\propto p_\theta(x_{n+1}|x_n)p_\theta(x_n|y_{0:n})$$

Given the approximation of  $p_\theta(x_n|y_{0:n})$  generated by the filtering in Eq. (8), one can find the following approximation:

$$p_\theta(x_n|y_{0:n}, x_{n+1}) \approx p_\theta(x_{n+1}|x_n)p(y_n|x_n) \sum_{i=1}^N p(x_n|x_{n-1}^i) \pi_{n-1}^i \quad (12)$$

where the weight is modified as:

$$\pi^i = \frac{w_i p(x_{n+1}|x_n^i)}{\sum_{j=1}^N w_j p(x_{n+1}|x_n^j)} \quad (13)$$

The detailed smoothing process is summarized as follows.

**Step 1.** Sample  $\{x_n^i\}_{i=1}^N$  via particle filtering.

**Step 2.** For each set of  $x_n^i$  and  $n=T-1, \dots, 1$ , resample  $x_n^i$  from  $\{x_n^i\}_{i=1}^N$  with weights  $\pi^i$ .

The PF and smoothing provide estimations of state variables  $x$  given a set of HR data, which will be further used in section III for parameter estimation and treadmill speed design.

#### D. Bayesian Parameter Estimation

Bayesian parameter estimation approach assigns a suitable prior density  $p(\theta)$  to  $\theta$  and infers the model parameters based on the posterior density  $p(x_{0:T}, \theta|y_{0:T})$ . The objective of the parameter estimation procedure is to maximize the log likelihood function as,

$$\max_\theta \log L(\theta) = \log \prod_{i=0}^T p(y_i|x_{0:i}, y_{0:i-1}) \quad (14)$$

In this study, we propose to use particle MCMC to seek the distributions of model parameters. Specifically, Particle Marginal Metropolis-Hastings (PMMH) sampler was used to sample from the proposal density [17]:

$$q((x_{0:T}^*, \theta^*)|(x_{0:T}, \theta)) = q(\theta^*|\theta)p(x_{0:T}^*|x_{0:T}) \quad (15)$$

where  $q(\theta^*|\theta)$  is a proposal density to obtain the next choice of  $\theta^*$  given  $\theta$  at the current location. The acceptance ratio for the joint proposal can be defined as [17]:

$$\min\left(1, \frac{p_{\theta^*}(y_{0:T})p(\theta^*)q(\theta|\theta^*)}{p_\theta(y_{0:T})p(\theta)q(\theta^*|\theta)}\right) \quad (16)$$

Note it is difficult to directly compute  $p_{\theta^*}(y_{0:T})$  and  $p_\theta(y_{0:T})$  with an acceptable probability. We choose to use PMMH sampler to estimate two likelihood terms. The approximation steps are summarized as follows.

First, given a set of model parameter  $\theta$ , the particle approximation of  $\hat{p}_\theta(y_{0:T})$  will be obtained.

Second, a proposal  $\theta^*$  is calculated by sampling from the Gaussian distribution with a mean value equals to the last value and an adaptively estimated covariance matrix.

Then, particle approximation  $\hat{p}_{\theta^*}(x_{0:T}^*|y_{0:T})$  and  $\hat{p}_{\theta^*}(y_{0:T})$  are obtained using the PF and smoother discussed in the previous section. One of the  $N$  particles is chosen based on the weight values as  $X_{0:T}^*$ . The chance for accepting the current  $\theta^*$  is approximated as:

$$\min\left(1, \frac{\hat{p}_{\theta^*}(y_{0:T})p(\theta^*)q(\theta|\theta^*)}{\hat{p}_\theta(y_{0:T})p(\theta)q(\theta^*|\theta)}\right) \quad (17)$$

The procedure repeats for  $M$  iterations until the likelihood function converges, and the posterior distribution of all parameters are characterized to obtain the optimal parameters.

#### D. Optimal Exercise Intensity

Further, given the optimally calibrated model, an optimal exercise intensity is identified based on the model prediction  $\hat{y}$  and a target heart rate  $HR_0$ . The optimal walking/running speed is determined via the optimization problem defined as follows:

$$\begin{aligned} \min_{u^*} \quad & \left\{ \frac{1}{T} (\hat{y} - HR_0)^2 \right\} \\ \text{s.t.} \quad & \hat{y} = g_\theta(x_t) + v_t \\ & x_t = f_\theta(x_{t-1}) + w_t \\ & 0 < u < 12 \end{aligned} \quad (18)$$

where  $\hat{y}$  is HR prediction between  $(t_0, t_0+T)$ , which can be calculated using Eqs. (1)-(6) in Section II A,  $HR_0$  is a user defined target HR.

### III. SIMULATIONS AND DESIGN OF EXPERIMENTS

#### A. Exercise Protocols

Two exercise protocols were considered in this work for model identification and exercise control design, respectively. The protocols are described as follow.

**Protocol 1** – Subject was at rest for the first 2.5 minutes and started to walk at a speed of 5km/hour for 15.5 minutes, then returned to resting state for 12 minutes. The same protocol was repeated with different walking/running speeds, i.e., 6 km/hour and 7 km/hour, respectively. The simulated data is shown in Fig. 1 (a). This protocol is determined following the previous study [9].

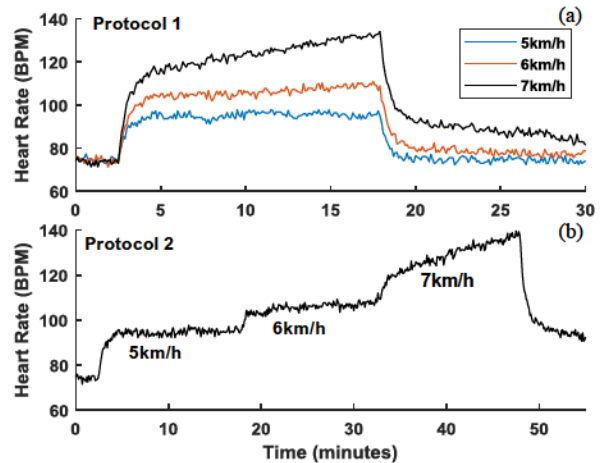


Figure 1. Heart Rate at different exercise protocols

**Protocol 2** – Subject was at rest for the first 2.5 minutes and started to walk at 5 km/hour for 15.5 minutes, then speeded up to more an intensive exercise, i.e., walking speed of 6km/hour for 15 minutes, and 7km/hour for another 15 minutes, before returning to the resting state. The simulated HR is shown in Fig. 1 (b).

## B. Simulation Experiments

HR was calculated using the state-space model given in Eqs. (1)-(6) with Euler method in a 0.1-minute time step. The state variables  $x_1$  and  $x_2$  were assumed to follow independent Gaussian distributions with zero means and covariances of 0.1 and 0.001, respectively. The noise in HR was considered to follow a normal distribution with zero mean and covariance of 1. Parameter estimation was performed following the steps discussed in Section II A-C, and 50 particles were used to compute state variables and search for model parameters. The optimization problem in exercise control was solved using genetic algorithm. All experiments were performed in MATLAB 2018b on a 64-bit Windows computer.

## IV. RESULTS

### A. Model Identification

In this section, the state-space HR model was optimized to fit simulated HR observations. The model parameters were estimated using multiple sets of HR observations, i.e., simulated HR at 5km/hour, 6km/hour, and 7 km/hour for 30 minutes (see Fig. 1 (a)). The noises in both state variables and HR observations were assumed to follow zero mean Gaussian distribution with different standard deviations, i.e.,  $\sigma_{x_1}=0.01$ ,  $\sigma_{x_2}=0.001$ , and  $\sigma_y=1$ . Given each set of observation, state variables  $x_t$  at time  $t$  was estimated through the PF and smoother with 50 particles. Initial values of the state variables were randomly generated from a normal distribution with mean value equals to 2 and variance equals to 1. It is worth mentioning that the filtering and smoothing are not sensitive to the changes in the initial value. The user can choose any values in a reasonable range. Given a set of parameters  $\theta$ , the likelihood  $p_\theta(y_{0:T})$  was calculated as the joint probability of all HR observations at  $t=0, \dots, T$ , which was further used in MCMC to determine the acceptance rate of the current attempt. Uniform prior distributions were assigned to all parameters with a lower bound of  $1e-6$  and upper bound equals to 5 times of the suggested parameters by [9]. The algorithm was initiated by sampling  $\theta$  from the prior distribution and proceeded with MCMC moves. A multivariate Gaussian distribution was used as the proposal distribution and the covariance function was updated iteratively as the algorithm proceeded. The algorithm was executed with  $T=300$  at 0.1 minutes time step for 1000 burn-in iterations and 5000 iterations. Estimated marginal posteriors for all model parameters  $p(\theta|y_{0:T})$  obtained from particle marginal Metropolis-Hastings are given in Fig. 2. The black vertical lines in Fig. 2 show the actual parameters, while the blue curves show the marginal posterior density of each parameter. As seen, some of the posterior densities have a Gaussian shape, whereas some follow non-Gaussian distribution. The proposed method can capture the true parameters, i.e., the mean of each posterior density is close to the actual parameter. Further, the actual parameter, the posterior mean and standard deviation are given in Table I.

TABLE I. SUMMARY OF PARAMETER ESTIMATION RESULTS

Parameters	$a_1$	$a_2$	$a_3$	$a_4$	$a_5$	$a_6$
True	1.84	24.32	0.0636	0.00321	8.32	0.38
Posterior Mean	1.93	24.99	0.0665	0.00331	8.33	0.38
Posterior s.d.	0.28	4.07	0.0128	0.0006	1.51	0.058

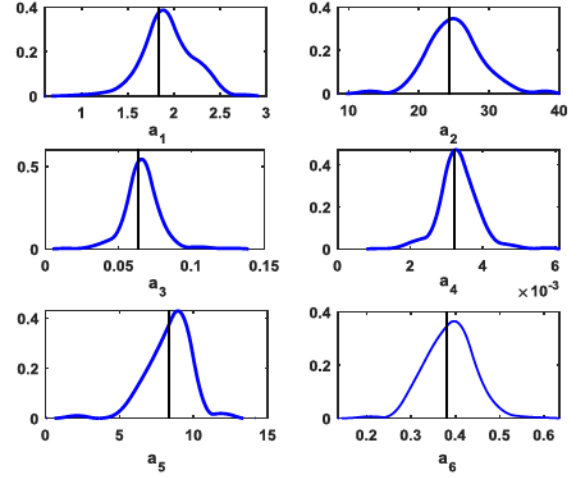


Figure 2. Estimated marginal posterior density of model parameters

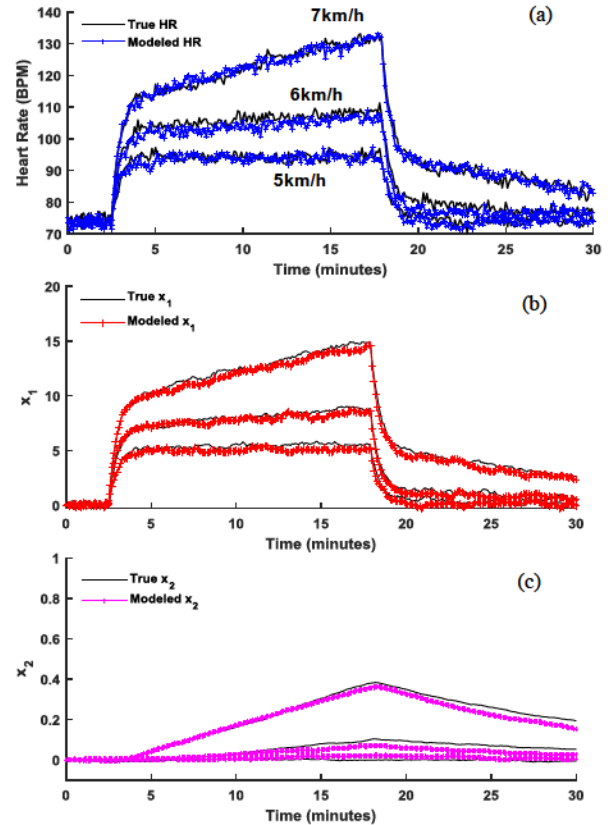


Figure 3. Modeled vs true heart rate (a), heart rate variations,  $x_1$  (b), peripheral effects,  $x_2$  (c)

In addition, using the identified model parameters with particle MCMC, the modeled HR and state variables by Eq. (1)-(6) at 5km/hour, 6km/hour, and 7km/hour are shown in Fig. 3, which are also compared to the true HR and state variables. As seen in Fig. 3, the modeled HR matches with actual HR, which demonstrates the accuracy of the estimated parameters. We further quantify the model error by calculating the average sum squared error (SSE) as:  $SSE = (1/3T) \sum_{u=5}^7 \sum_{t=1}^T (\hat{y}_{u,t} - y_{u,t})^2$ . The average SSE between modeled HR and true HR for all the three speed is 1.38 beat per minute (BPM), and the average SSE between modeled state variables and true state values are  $SSE_{x1} = 0.04$  and  $SSE_{x2}$



= 0.0001. The average SSEs for both two state variables are less than the standard deviation of noise, i.e.,  $\sigma_{x_1}=0.01$ ,  $\sigma_{x_2}=0.001$ . Therefore, the identified model is acceptable and will be further used for the treadmill speed optimization in the following Section.

### B. Optimal Treadmill Speed Identification

The treadmill speed optimization is accomplished in two steps, i.e., HR modeling and tracking, and optimal speed identification. We assume HR signals for  $t_0$  minutes prior the current time can be collected, but the state variables and the starting values are unknown. Given the optimally calibrated model, we first apply PF and smoother to estimate the state variables up to  $t_0$  minutes. Then, the optimal walking/running speed in the next  $T$  minutes will be calculated through the optimization defined in Eq. 18. Further, the optimal speed will be given as an input to the HR model to predict the HR changes for the next  $T$  minutes, which will be compared with the target HR for validation. The modeling and optimization results are shown as follows.

**HR tracking.** We assume a subject started the exercise at unknow time, and HR signals are recorded at  $t=0$  for  $t_0=30$  minutes. The simulated observations are plotted in Fig. 4 (see the black lines in Fig. 4 for HR observations). The data was generated following the 2<sup>nd</sup> protocol given in Section III. The signals were recorded a few minutes after the exercise started. Given the HR data and the model obtained from the previous section, we first applied PF to track the HR variations. Random initial values of the state variables  $x_1$  and  $x_2$  were generated from two normal distributions, i.e.,  $x_1^0 \sim N(5, 10^2)$  and  $x_2^0 \sim N(0.02, 0.01^2)$ . The parameters of the distributions were determined based on the possible ranges of the two variables. The HR signals, and the state variables  $x_1$  and  $x_2$  estimated with PF given random starting values are shown in Fig. 4, which are compared with the true values (black line).

As see in Fig. 4 (a), the blue line shows the HR calculated from the PF and the HR model. It is found that the difference between modeled HR and true HR is large for the first 5 minutes. This is due to the random guess on the initial values of state variables. After the first 5 minutes, the modeled HR approaches to the true observations, which demonstrates the efficiency of PF for tracking HR responses. Similar observations can be found for the two state variables  $x_1$  and  $x_2$  (see the red and purple lines in Fig. 4 (a) and (b)). Additionally, larger errors in  $x_2$  are observed between 15 to 20 minutes, which is due to the change of treadmill speed, i.e., the running speed was increased from 5 km/hour to 6 km/hour at 15 minutes. In addition, the modeled HR at  $t_0=30$  minutes was 106.9 BPM, and the actual value is 106.5 BPM. The estimated state variables are:  $\hat{x}_1^{t_0}=8.038$  BPM and  $\hat{x}_2^{t_0}=0.0594$ , respectively, which are close to the actual values, i.e.,  $x_1^{t_0}=7.931$  BPM and  $x_2^{t_0}=0.088$ . Note that 100 particles were used to track the actual HR in this case study. The number of particles could affect the modeling accuracy, and increasing particle numbers can further improve the prediction accuracy. However, due to space limits, this is not discussed in this work. Given the estimations of state variables at  $t_0$ , we further applied the HR model to predict future HR at different treadmill speeds and find the optimal speed that can elevate or lower HR to a target value  $HR_0$ .

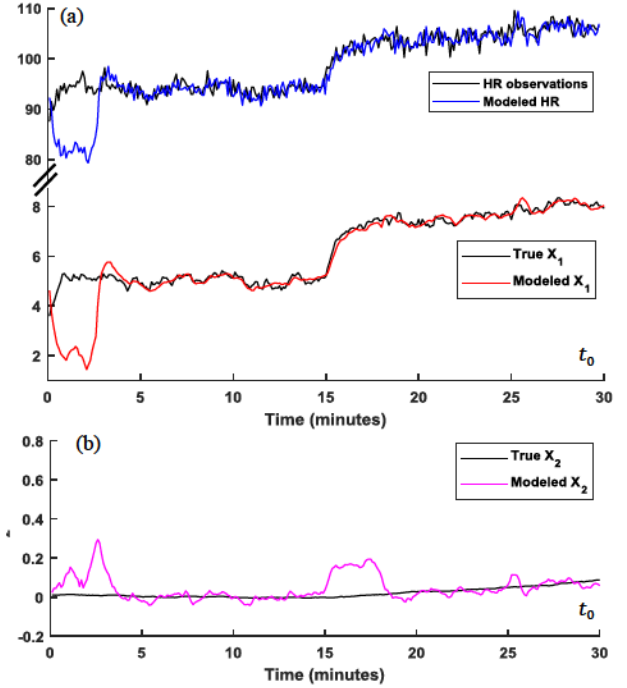


Figure 4 HR observations vs modeled HR by particle filter and smoother

**Optimal Treadmill Speed Identification.** We further performed different experiments using three target HR values, i.e.,  $HR_0=100$  BPM, 120 BPM, and 140 BPM, respectively. The objective is to raise or decrease the HR so that the average HR in the future  $T$  minutes can be as close as possible to the target value. Given a target HR and state variables at  $t_0=30$  minutes, HR in  $T$  minutes were calculated using the model given in Eq. (1)-(6) and the optimal parameters identified in previous sections. The best speed was identified by minimizing the sum-squared error between HR predictions and the target HR (see Eq. 18) for all time steps between  $t_0$  to  $t_0+T$  minutes. We set  $T=15$  minutes, and HR predictions were calculated for every 0.1 minute. Genetic algorithm was used to solve the optimization, because there are multiple local optimal solutions to the optimization problem, and both HR observations and model predictions involve noises and uncertainty, which consequently introduces noise into the objective function [19]. However, different optimization technique can be explored to find the optimal solution.

The optimal solutions of  $u^*$  with different target HRs are summarized in Table II. As seen, the best running speeds that raise HR to 120 BPM and 140 BPM are 6.62 km/hour and 7.82 km/hour, respectively. The optimal speed that reduces the HR to 100 BPM is 5.29 km/hour. HR changes at the three treadmill speeds after  $t_0$  are shown in Fig. 5. As seen in Fig. 5, the black line and the blue line between  $t=0$  and 30 show the HR observations and the modeled HR, respectively. The HR control starts at  $t_0=30$  minutes when the initial speed is 6 km/hour. When the treadmill speed is set to 7.82 km/hour, the HR raises rapidly in a few minutes to 130~140BPM. The increasing trend continues until time reaches about 45 minutes, when the HR is increased to 150 BPM (see the green line in Fig. 5). In addition, when the treadmill speed is set to 6.62 km/hour, HR increases rapidly to about 118 BPM in a

couple of minutes, and then continues to raise at a mild rate. By the end of 45 minutes, HR reaches to about 130 BPM. Whereas, when speed is set to 5.28 km/hour, which is lower than the current speed, HR decreases to 100 BPM in a few minutes and stabilizes at 100 BPM until the end of the simulations. The performance of the proposed speed control algorithm is also quantitatively studied using two parameters, i.e. error between the average HR in time window  $T$  and target HR (i.e., AveError), and average of the absolute error (i.e., Ave SAE). As see in Table II, AveErrors for the target HR of 140, 120, and 100 BPM are 1.015, 2.836, and 1.951 BPM, respectively, and average SAE for the three targets are 6.60, 4.40, and 2.45 BPM (see Table II). Lower AveError is observed for  $HR_0=140$ BPM, because HR response evenly distribute on both side of 140BPM at 30 ~ 45 minutes. This makes the average in the time window to be very close to the target value. In addition, lower SAE is observed for  $HR_0=100$ BPM because HR shows smaller variance around 100 BPM. The suboptimal performance of the controller at target HRs of 140BPM and 120BPM may be due to the fact that the controller does not consider the rate of speed changes and favors a solution that raises HR to the target value as fast as possible. To improve the performance, penalization can be included to regulate speed changes.

TABLE II. SUMMARY OF OPTIMAL SPEED DESIGN WITH EQ. (17)

$HR_0$ (BPM)	Treadmill Speed (km/hour)	AveError	Ave SAE
140	7.82	1.015	6.60
120	6.62	2.836	4.40
100	5.29	1.951	2.45

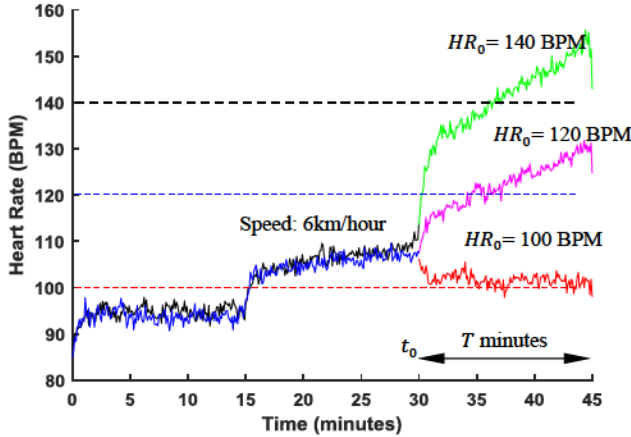


Figure 5. HR at optimal treadmill speeds identified at three target  $HR_0$

## V. CONCLUSION

HR is one of the most important cardiovascular variables that can be easily measured and provide significant insights of cardiac functions during physical exercise. This paper presents a new modeling and control framework to optimally calibrate a state-space HR model, and further uses the model to suggest optimal exercise intensity in order to meet different training goals. Specifically, particle filter (PF) is used for both model calibration and optimal treadmill speed identification. The advantage of using PF is that it copes with nonlinear non-Gaussian systems with unknown initial states. The proposed

method is validated through simulation studies, which demonstrates its feasibility and efficiency for HR modeling, tracking, and optimal exercise intensity identification. This shows a great potential of the present method in advancing both cardiovascular health and cardiac healthcare.

## ACKNOWLEDGMENT

This project is partially supported by NSF CMMI-1646664, CMMI-1728338, and CMMI-1727487

## REFERENCES

- [1] E. J. Benjamin *et al.*, "Heart Disease and Stroke Statistics-2017 Update: A Report From the American Heart Association," *Circulation*, vol. 135, no. 10, pp. e146-e603, 2017.
- [2] N. CDC. Underlying Cause of Death 1999-2013 on CDC WONDER Online Database, released 2015. [Online].
- [3] M. S. Zakythinaki, "Simulating heart rate kinetics during incremental and interval training," (in English), vol. 8, no. 1, p. 144, 2016.
- [4] X. Jouven, J.-P. Empana, P. J. Schwartz, M. Desnos, D. Courbon, and P. Ducimetière, "Heart-Rate Profile during Exercise as a Predictor of Sudden Death," *New England Journal of Medicine*, vol. 352, no. 19, pp. 1951-1958, 2005.
- [5] K. P. Savonen *et al.*, "Heart rate response during exercise test and cardiovascular mortality in middle-aged men," (in eng), *Eur Heart J*, vol. 27, no. 5, pp. 582-8, Mar 2006.
- [6] M. Hájek, J. Potůček, and V. Brodán, *Mathematical model of heart rate regulation during exercise*. 1980, pp. 191-195.
- [7] J. Robert Stirling, M. Zakythinaki, I. Román, and J. Sampedro, *A Model of Heart Rate Kinetics in Response to Exercise*. 2008, pp. 426-436.
- [8] S. W. Su, L. Wang, B. G. Celler, A. V. Savkin, and Y. Guo, "Identification and Control for Heart Rate Regulation During Treadmill Exercise," *IEEE Transactions on Biomedical Engineering*, vol. 54, no. 7, pp. 1238-1246, 2007.
- [9] T. M. Cheng, A. V. Savkin, B. G. Celler, S. W. Su, and L. Wang, "Nonlinear modeling and control of human heart rate response during exercise with various work load intensities," (in eng), *IEEE Trans Biomed Eng*, vol. 55, no. 11, pp. 2499-508, Nov 2008.
- [10] J. A. Suykens and J. Vandewalle, "Recurrent least squares support vector machines," *IEEE Transactions on Circuits and Systems I: Fundamental Theory and Applications*, vol. 47, no. 7, pp. 1109-1114, 2000.
- [11] T. C. Hsia, *System identification: least-squares methods*. Lexington books Lexington, 1977.
- [12] F. Ding and T. Chen, "Hierarchical gradient-based identification of multivariable discrete-time systems," *Automatica*, vol. 41, no. 2, pp. 315-325, 2005/02/01/ 2005.
- [13] V. Verdult, L. Ljung, and M. Verhaegen, "Identification of composite local linear state-space models using a projected gradient search," *International Journal of Control*, vol. 75, no. 16-17, pp. 1385-1398, 2002.
- [14] T. A. Johansen, "On Tikhonov regularization, bias and variance in nonlinear system identification," *Automatica*, vol. 33, no. 3, pp. 441-446, 1997.
- [15] Y. Zhang, "Unbiased identification of a class of multi-input single-output systems with correlated disturbances using bias compensation methods," *Mathematical and Computer Modelling*, vol. 53, no. 9-10, pp. 1810-1819, 2011.
- [16] M. K. Pitt and N. Shephard, "Filtering via Simulation: Auxiliary Particle Filters," *Journal of the American Statistical Association*, vol. 94, no. 446, pp. 590-599, 1999/06/01 1999.
- [17] N. Kantas, A. Doucet, S. S. Singh, J. Maciejowski, and N. Chopin, "On particle methods for parameter estimation in state-space models," *Statistical science*, vol. 30, no. 3, pp. 328-351, 2015.
- [18] S. J. Godsill, A. Doucet, and M. West, "Monte Carlo smoothing for nonlinear time series," *Journal of the american statistical association*, vol. 99, no. 465, pp. 156-168, 2004.
- [19] "Genetic Algorithms," in *Wiley Encyclopedia of Computer Science and Engineering*, pp. 1-15.